Nuclear Materials and Energy 12 (2017) 720–724

Contents lists available at ScienceDirect

Nuclear Materials and Energy

journal homepage: www.elsevier.com/locate/nme

Elimination of inter-discharge helium glow discharge cleaning with lithium evaporation in NSTX

R. Maingi[a,*], R. Kaita[a], F. Scotti[b], V.A. Soukhanovskii[b], the NSTX team

[a] Princeton Plasma Physics Laboratory, Receiving 3, Route 1 North, Princeton, NJ 08543 USA
[b] Lawrence Livermore National Laboratory, 7000 East Ave, P.O. Box 808, Livermore CA 94551, USA

ARTICLE INFO

Article history:
Received 13 July 2016
Revised 12 March 2017
Accepted 26 March 2017
Available online 4 April 2017

Keywords:
NSTX
Lithium
Recycling
Pedestal
Energy confinement

ABSTRACT

Operation in the National Spherical Torus Experiment (NSTX) typically used either periodic boronization and inter-shot helium glow discharge cleaning (HeGDC), or inter-shot lithium evaporation without boronization, and initially with inter-shot HeGDC. To assess the viability of operation without HeGDC, dedicated experiments were conducted in which Li evaporation was used while systematically shrinking the HeGDC between shots from the standard 10 min to zero (10→6.5→4→0). Good shot reproducibility without HeGDC was achieved with lithium evaporations of 100 mg or higher; evaporations of 200–300 mg typically resulted in very low ELM frequency or ELM-free operation, reduced wall fueling, and improved energy confinement. The use of HeGDC before lithium evaporation modestly reduced D_α in the outer scrape-off layer, but not at the strike point. Pedestal electron and ion temperature also improved modestly, suggesting that HeGDC prior to lithium evaporation is a useful tool for experiments that seek to maximize plasma performance.

1. Introduction

Fusion devices use a variety of techniques [1] to manage the intense plasma-wall interactions [2] that can reduce plasma performance and/or can damage the wall materials. Two such techniques are the use of wall coatings [3], applied infrequently or sometimes between discharges, and the use of discharge conditioning between plasma discharges, e.g. helium glow discharge cleaning (HeGDC) [4]. On the National Spherical Torus Experiment (NSTX), helium glow discharge cleaning was routinely used in conjunction with periodic boronizations to reduce oxygen content [5,6] and provide routine access to H-mode [7]. These early studies of boronized plasmas with inter-discharge HeGDC were followed by studies of lithium injection, first via pellets [8], and then via evaporation [9]. The evaporative coatings showed an increase in energy confinement [10,11], and elimination of Type I ELMs [12], related to reduced wall fueling and an inward shift of the pedestal density and pressure profiles [13,14]. While the first of these experiments used HeGDC prior to lithium evaporation, the wall fueling reduction afforded by lithium evaporation [15] raised the prospect of eliminating HeGDC altogether, to simplify operational procedures and reduce the time between discharges. To test this, a sequence of discharges was conducted with the HeGDC time before lithium evaporation reduced sequentially from 10 min down to zero, at approximately constant lithium dose, external heating, and fueling. The remainder of this paper describes this systematic HeGDC scan.

2. Layout of wall conditioning tools and previous treatments for wall conditioning

The NSTX plasma-facing components (PFCs) were made of graphite, either ATJ or carbon-fiber composite, and of varying thicknesses from 1.3 to 5.1 cm [16]. Two wall-mounted anodes were typically used as the HeGDC electrodes for NSTX, separated toroidally by roughly 120° (Fig. 1a) [5]. The pair of electrodes typically drew ~3 A of current at an applied voltage of 400–500 V, with a He fill pressure ~3–4 mTorr. Typical HeGDC duration was ~10 min, followed by a few minutes for pump out, and then a 15 min inter-discharge cycle time. Longer HeGDC durations were tested up to 15 min, with a 20 min inter-discharge cycle time, for experiments that desired the lowest recycling conditions with boronized wall conditions. It should be noted that boronization with tri-methyl boron, which was performed approximately once per month in NSTX, used the same HeGDC system, with a mixture of He and tri-methyl boron injected at a port near the pumping duct [5]. Reproducible ELMy H-mode discharges were obtained in

* Corresponding author.
E-mail address: rmaingi@pppl.gov (R. Maingi).

http://dx.doi.org/10.1016/j.nme.2017.03.034

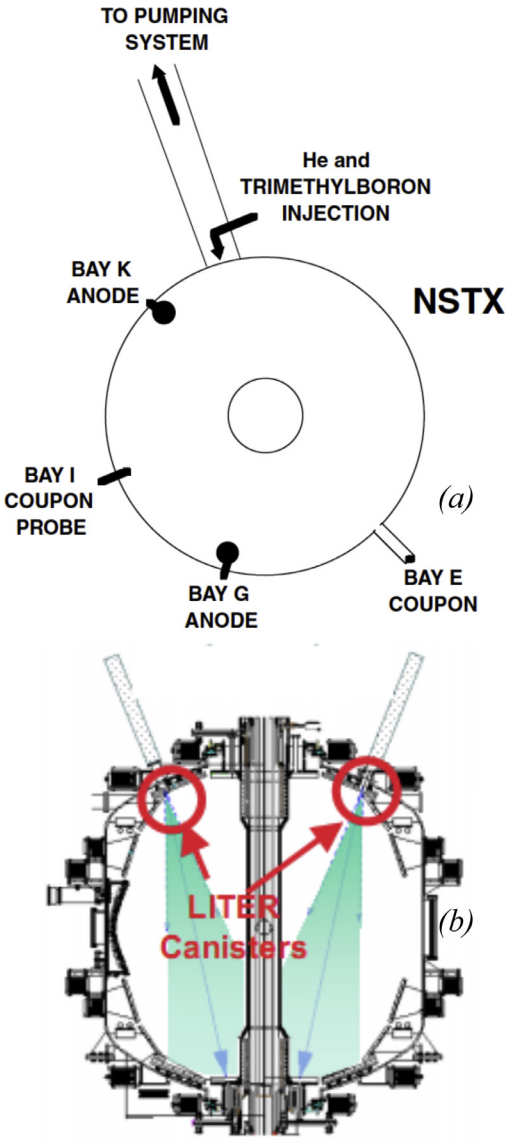

Fig. 1. (a) plan view of NSTX showing the location of two HeGDC probes used as anodes; (b) poloidal cross-section of NSTX showing two (toroidally separated) lithium evaporators, and the Gaussian width spread of the evaporation cone.

NSTX, including ones with Type I ELMs [17], using these wall conditioning techniques of periodic boronizations and inter-discharge HeGDC.

An important research element in NSTX was to evaluate the effect of lithium coatings on the carbon PFCs. Initial experiments were done with a single lithium evaporator, which were then extended to two evaporators separated toroidally by about roughly 150° (Fig. 1b) [9]. These evaporators deposited lithium in a Gaussian distribution with a 1/e fall-off 11.5° away from the centerline. The deposition rate could be varied between 10 and 70 mg/min/evaporator, by changing the evaporator operating temperature. A typical discharge sequence used 6.5–10 min of HeGDC, followed by 7–8 min of lithium evaporation, leading to a ~20 min inter-discharge cycle time. It was found that the Type I ELMs were methodically eliminated [12] and confinement was progressively improved [18] with increasing lithium dose. While these first experiments were conducted with the combination of HeGDC followed by lithium evaporation, a dedicated experiment in which the HeGDC duration was systematically reduced from 10 min to zero at constant lithium evaporation was conducted, as described below.

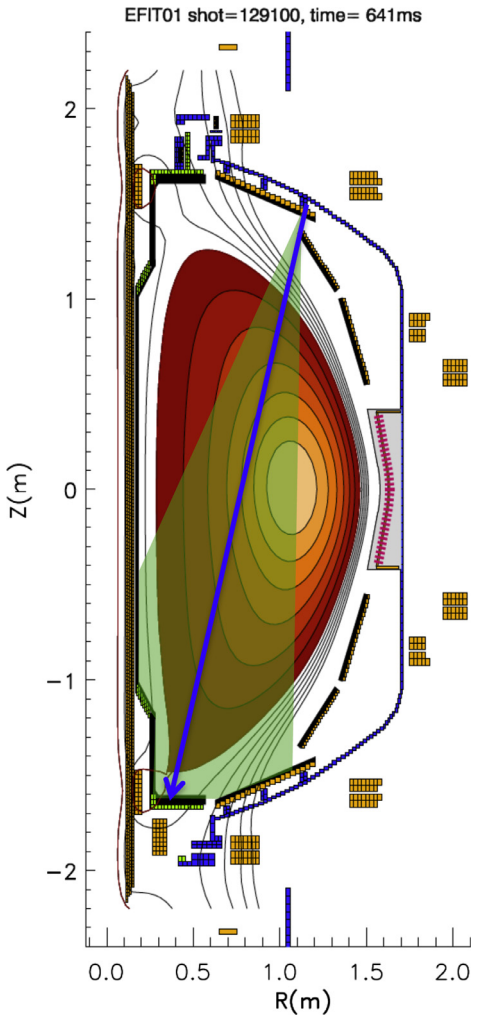

Fig. 2. boundary equilibrium shape with centroid of lithium evaporator deposition for representative discharge from experiment.

3. Effects of lithium evaporation on wall fueling and local recycling

The HeGDC duration variation experiment was conducted in highly shaped plasmas: average triangularity $\delta \sim 0.6$–0.7, elongation $\kappa \sim 2.2$, high squareness, in a near double-null configuration (Fig. 2). This configuration was partly chosen because the centroid of the lithium evaporation was close to the outer strike point, which was shown in subsequent experiments to be more effective at reducing wall fueling than configurations where the outer strike point was far from the centroid of lithium deposition [19]. Other discharge parameters were plasma current $I_p = 0.9$ MA, toroidal field $B_t = -0.45$ T, ion grad-B drift toward the lower X-point, neutral beam power (P_{NBI}) between 4 and 6 MW (although all direct comparisons are made during the 4 MW phases of discharges), and constant external gas fueling.

A comparison of discharge evolution from several relevant discharges with identical external gas fueling is shown in Fig. 3. A reference ELMy H-mode, with no lithium evaporation, and taken before any lithium had been deposited in the campaign (129014–black solid) is compared with a similar discharge (129096–red dashed) with no direct lithium evaporation (but with 19 g of intervening lithium evaporation), and a discharge with ~ 500 mg of lithium evaporation and with 6.5 min of HeGDC prior to lithium evaporation (129101–blue dash dot). Each of these discharges had phases of 4 MW and 6 MW of neutral beam injection

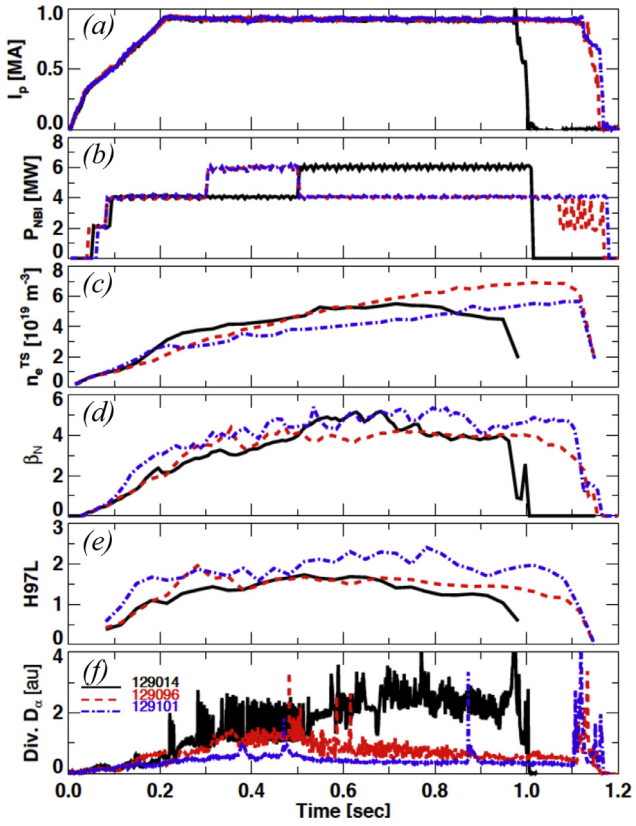

Fig. 3. evolution of discharge quantities for three discharges: (a) plasma current I_p, (b) neutral beam heating power P_{NBI}, (c) line-averaged density from Thomson Scattering n_e^{TS}, (d) normalized plasma pressure β_N, (e) energy confinement relative to ITER H97 L-mode scaling, and (f) lower divertor D_α. See the text for description of discharges.

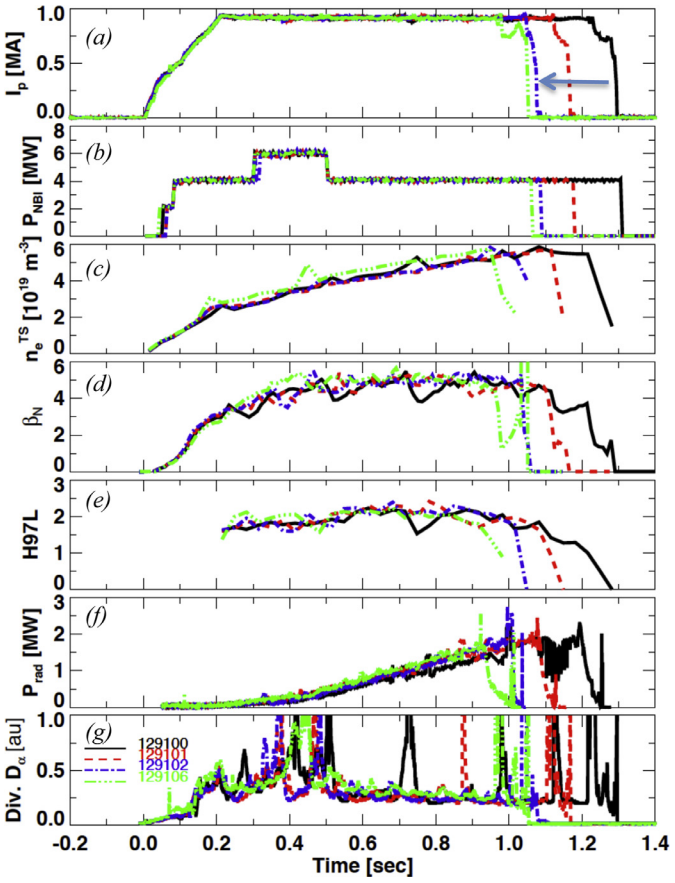

Fig. 4. evolution of discharge quantities for discharges during HeGDC duration scan: (a) plasma current I_p, (b) neutral beam heating power P_{NBI}, (c) line-averaged density from Thomson Scattering n_e^{TS}, (d) normalized plasma pressure β_N, (e) energy confinement relative to ITER H97 L-mode scaling, (f) core radiated power P_{rad}, and (g) lower divertor D_α. The duration of HeGDC preceding Li evaporation decreased in the direction of the arrow in panel (a). The color coding is: 10 min HeGDC (black), 6.5 min HeGDC (red), 4 min HeGDC (blue), and no HeGDC (green). (For interpretation of the references to color in this figure legend, the reader is referred to the web version of this article.)

(panel (b) - P_{NBI}). The line-average density from Thomson scattering (panel (c)) ramped in all 3 discharges but had the slowest temporal evolution in the one with Li evaporation with preceding HeGDC. β_N, the normalized pressure, is defined as $\beta_N = \beta_t B_t a_m / I_p$, where β_t is the average plasma pressure normalized to the on-axis vacuum toroidal field: $\beta = 4\mu_0 W_{MHD}/(3V_p B_t^2)$. Here B_t is the toroidal field, a_m the minor radius, W_{MHD} the stored energy from equilibrium reconstructions, V_p the plasma volume, and μ_0 the permittivity of free space. Panel (d) shows that β_N was highest for the discharge with Li and preceding HeGDC, when comparing the 4 MW P_{NBI} phases. This is also reflected in the energy confinement time, τ_E, normalized to the H97L L-mode scaling [20] (panel (e)). Panel (f) shows that the lower divertor D_α emission is reduced substantially by the presence of lithium in NSTX (i.e. red dash curve lower than black solid curve), and further reduced with application of lithium and HeGDC prior to the discharge. ELM elimination, however, requires the lithium evaporation just before the discharge.

4. Scan of HeGDC duration preceding Li evaporation

A systematic scan of the HeGDC time prior to lithium evaporation was conducted, by going from 10 min to 6.5 min to 4 min and then eliminating HeGDC completely. The starting point was an ELM-free H-mode with ~ 500 mg lithium pre-discharge evaporation. A comparison of several of the discharges from the HeGDC duration scan is shown in Fig. 4. As can be seen, the plasma evolution was very similar in these discharges, although the reduction of the HeGDC duration at fixed external fueling resulted in a modest decrease of the observed pulse lengths (panel (a)). The discharge with no HeGDC (#129106 green curves) did have slightly higher radiated power (P_{rad}) and divertor D_α emission (panels (f) and (g)).

The edge electron density, temperature, and ion temperature (n_e, T_e, T_i) profiles at the same line-averaged density are compared for three of the discharges during the HeGDC duration scan in Fig. 5. Panel 5(a) confirms that the density profile shape and magnitude was nearly identical for the three chosen time slices. A reduction in the edge T_e and T_i of up to 15–30% can be observed in panels (b) and (c), with the biggest reduction observed for the discharge with no HeGDC (#129106 blue diamonds).

As can be seen in panel 4(g), the divertor D_α emission is slightly higher when HeGDC was completely omitted prior to lithium evaporation. The divertor D_α emission radial profile is compared in Fig. 6 for the discharges from Fig. 4 at a representative time, t = 0.55 s. It can be seen that the peak emission near the outer strike point, i.e. at radius ~ 0.35 m is comparable for the discharges, but that the emission from radius > 0.45 m is markedly higher for the discharge without HeGDC (#129106 – green). We note that the profiles at other times showed these same trends.

To quantify the impact of the radial variations on the total flux, the photon flux was converted to equivalent local ion flux by $\Gamma = \gamma \int_{R1}^{R2} D_\alpha(r) 2\pi R(r) dr$, where γ is the number of ionizations per photon (assumed to be 20 for an ionizing plasma), for several discharges from the previous figures. We note that the approx-

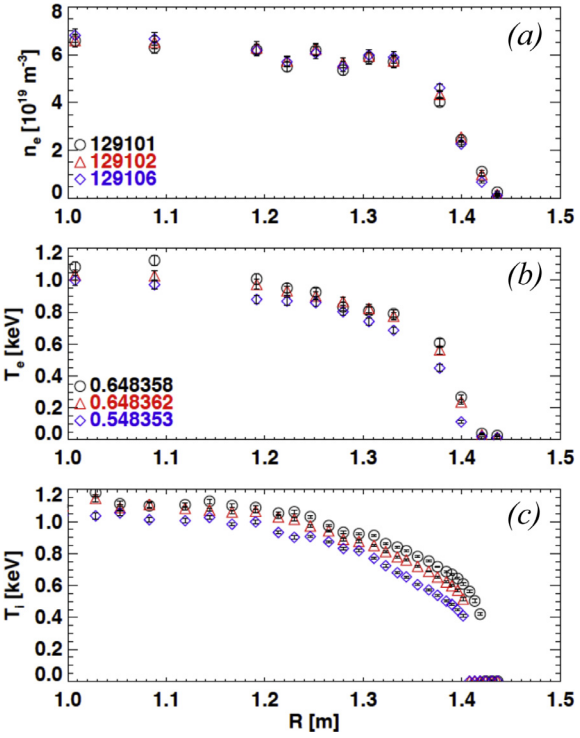

Fig. 5. comparison of n_e, T_e, and T_i profiles for discharges with 6.5 min HeGDC (black circles), 4 min HeGDC (red triangles), and no HeGDC (blue diamonds). All discharges were followed by comparable amounts of lithium evaporation. The legends in panels (a) and (b) list shot numbers and times used for Thomson profiles. (For interpretation of the references to color in this figure legend, the reader is referred to the web version of this article.)

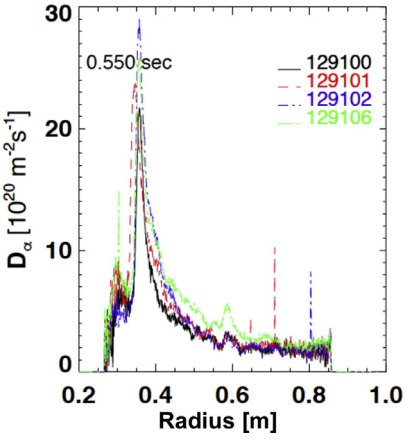

Fig. 6. radial profile of D_α emission from discharge with 10 min HeGDC (black), 6.5 min HeGDC (red), 4 min HeGDC (blue) and no HeGDC (green). All discharges were followed by comparable amounts of lithium evaporation. (For interpretation of the references to color in this figure legend, the reader is referred to the web version of this article.)

imation of 20 ionizations per D_α photon is necessary because divertor n_e and T_e are unavailable for this dataset; the range is 10–30 ionizations per D_α photon for typical divertor conditions, and thus this approximation is semi-quantitative at best. Fig. 7 compares the time evolution of the fluxes for the far SOL profiles (i.e. R1 = 0.45 m, R2 = 0.55 m, panel (a)) and the near SOL fluxes (i.e. R1 = 0.35 m, R2 = 0.45 m, panel (b)). As can be seen in Fig. 7a, the far SOL particle flux is higher for the discharge without HeGDC (#129106 green) than the ones with 6.5 min HeGDC (129102 blue) and 10 min HeGDC (129100 black). For context, the flux from the discharge with no lithium evaporation and 10 min HeGDC (#129096 orange) is also plotted. Fig. 7b shows that the near SOL

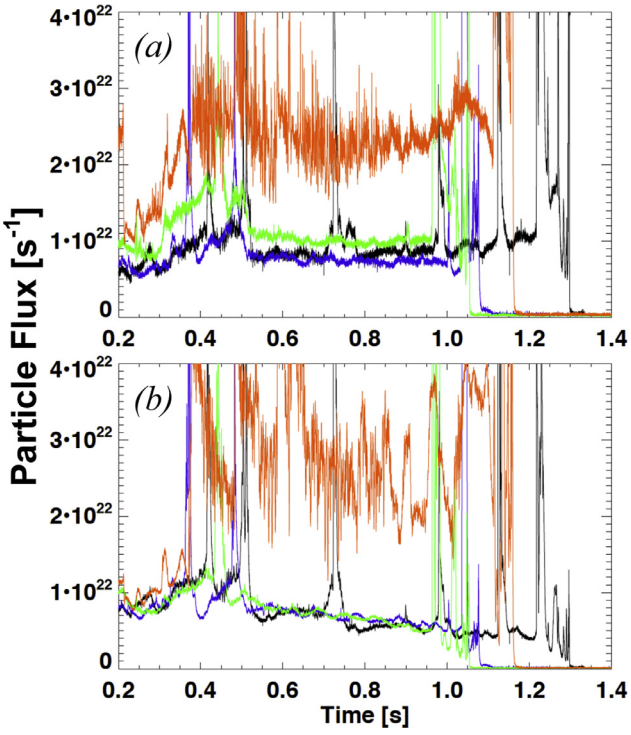

Fig. 7. Equivalent particle flux by integrating D_α emission in (a) far SOL, and (b) near SOL, from discharges with 10 min HeGDC (black), 6.5 min HeGDC (blue), and no HeGDC (green). Also shown is a discharge with 10 min HeGDC but no Li dose (orange). See the text for additional information. (For interpretation of the references to color in this figure legend, the reader is referred to the web version of this article.)

particle flux for the three discharges with lithium evaporation are comparable, and all are much lower than for the discharge with no lithium evaporation. One speculation for the similarity in the near SOL flux is that the intense plasma-bombardment near the outer strike point tends to saturate and regulate the surface rapidly, i.e. largely independent of the the preceding HeGDC. One possible mechanism for this is that the high PFC temperature near the strike point may hasten the diffusion rate from the bulk back to the surface. However the lower flux in the far SOL for discharges with HeGDC means that the equilibrium surface particle flux can be affected in low fluence zones, i.e. that the HeGDC can reduce D_α in those regions. It is interesting to note that the flux reduction does not depend on the duration of HeGDC, i.e. deployment of small durations is sufficient for flux control.

There is a natural tendency for the D_α emission to be equated to recycling, i.e. high D_α = high recycling. Defining the "local recycling coefficient" as the ratio of D_α emission ("outflux from the target") to local ion saturation current from an embedded Langmuir probe ("influx to the target), we find that the "local recycling coefficient" does not change with the HeGDC duration. However if "recycling" is viewed as the ratio of D_α emission to external fueling, then indeed the discharge with no HeGDC exhibits higher "recycling" than the ones with preceding HeGDC. Thus these results cannot be generically interpreted as "HeGDC reduced recycling", because the quantification of "recycling" is both difficult and variable depending on the definition.

5. Summary and conclusions

We have conducted a systematic scan of the HeGDC time, applied before lithium evaporation, in NSTX. At constant external fueling and lithium evaporation, the discharge duration shrank modestly with decreasing HeGDC duration. Moreover the edge

T_e and T_i decreased moderately with decreasing HeGDC duration at constant density and heating power. On the other hand, the divertor D_α emission in the far SOL increased when HeGDC was eliminated, but was otherwise unaffected by HeGDC duration. Moreover the near-SOL divertor D_α emission was unaffected by the duration of HeGDC. Finally with the ~500 mg of lithium dose deployed, all discharges were ELM-free, also independent of the HeGDC duration.

These results have practical implications for NSTX-U [21]. A cycle of 3–5 min HeGDC, followed by ~10 min of lithium evaporation is advocated, as that fits efficiently within the typical inter-discharge cycle time of 15–20 min. On the other hand, experiments that desire the highest performance discharges should deploy longer HeGDC times, albeit at the cost of increasing the inter-dicharge cycle time.

Acknowledgments

This research was sponsored in part by U.S. Dept. of Energy under contracts DE-AC02-09CH11466, DE-AC05-00OR22725, and DE-AC52-07NA27344. We gratefully acknowledge discussions with C.H. Skinner, and the contributions of the NSTX operations staff.

References

[1] J. Winter, Plasma Phys. Control. Fusion 38 (1996) 1503.
[2] G. Federici, C.H. Skinner, J.N. Brooks, et al., Nucl. Fusion 41 (2001) 1967.
[3] J. Winter, Plasma Phys. Control. Fusion 36 (1994) B263.
[4] G.L. Jackson, T.S. Taylor, P.L. Taylor, Nucl. Fusion 30 (1990) 2305.
[5] C.H. Skinner, H.W. Kugel, R. Maingi, et al., Nucl. Fusion 42 (2002) 329.
[6] H.W. Kugel, V. Soukhanovskii, M. Bell, et al., J. Nucl. Mater. 313 (2003) 187.
[7] R. Maingi, M. Bell, R. Bell, et al., Phys. Rev. Lett. 88 (2002) 035003.
[8] H.W. Kugel, M.G. Bell, R. Bell, et al., J. Nucl. Mater. 363–365 (2007) 791.
[9] H.W. Kugel, D. Mansfield, R. Maingi, et al., J. Nucl. Mater. 390–391 (2009) 1000.
[10] H.W. Kugel, M.G. Bell, J.-W. Ahn, et al., Phys. Plasmas 15 (2008) 056118.
[11] M.G. Bell, H.W. Kugel, R. Kaita, et al., Plasma Phys. Control. Fusion 51 (2009) 124054.
[12] D.K. Mansfield, H.W. Kugel, R. Maingi, et al., J. Nucl. Mater. 390–391 (2009) 764.
[13] R. Maingi, T.H. Osborne, B.P. LeBlanc, et al., Phys. Rev. Lett. 103 (2009) 075001.
[14] J.M. Canik, R. Maingi, S. Kubota, et al., Phys. Plasmas 18 (2011) 056118.
[15] J.M. Canik, R. Maingi, V.A. Soukhanovskii, et al., J. Nucl. Mater. 415 (2011) S409.
[16] H.W. Kugel, R. Maingi, W. Wampler, et al., J. Nucl. Mater. 290–293 (2001) 1185.
[17] R. Maingi, C.E. Bush, E.D. Fredrickson, et al., Nucl. Fusion 45 (2005) 1066.
[18] R. Maingi, S.M. Kaye, C.H. Skinner, et al., Phys. Rev. Lett. 107 (2011) 145004.
[19] R. Maingi, T.H. Osborne, M.G. Bell, et al., J. Nucl. Mater. 463 (2015) 1134.
[20] S.M. Kaye, and the ITER Confinement Database Working Group, Nucl. Fusion 37 (1997) 1303.
[21] J.E. Menard, S. Gerhardt, M. Bell, et al., Nucl. Fusion 52 (2012) 083015.